ACS Catalysis

Research Article

pubs.acs.org/acscatalysis

# Brookite vs Anatase $TiO_2$ in the Photocatalytic Activity for Organic Degradation in Water

Zhen Li, Shan Cong, and Yiming Xu*

State Key Laboratory of Silicon Materials and Department of Chemistry, Zhejiang University, Hangzhou 310027, Zhejiang, China

Supporting Information

**ABSTRACT:** Brookite is the least studied $TiO_2$, and its photocatalytic activity higher or lower than that of anatase still remains unclear. In this work, three different model reactions have been used for the activity assessment. Phase-pure brookite and anatase were homemade at different temperatures ($T_s$ = 200−500 °C), as confirmed by X-ray diffraction and Raman spectroscopy. For phenol oxidation in aerated aqueous solution, brookite showed an apparent activity higher and lower than that of anatase at low and high $T_s$, respectively. For chromate reduction in aerated aqueous suspension, the apparent activity of brookite was always lower than that of anatase. However, with the same amount of Cr(VI) or Ag(I) adsorbed on the oxide in water for Cr(VI) reduction or for phenol degradation under $N_2$, the intrinsic activities of brookite and anatase not only became similar at given $T_s$ but also increased with the increase of $T_s$. Moreover, for $O_2$ reduction to $H_2O_2$ in the presence of excess phenol, the BET surface area normalized activity of brookite was always higher than that of anatase, the trend of which was similar to that observed from phenol degradation in aerated aqueous solution. It is proposed that brookite has a stronger affinity to $O_2$ in water than anatase. Then, the observed difference between brookite and anatase in the apparent photocatalytic activity for phenol degradation is ascribed to the combined effect of $T_s$, surface area, and sorption capacity toward the dissolved $O_2$ in water.

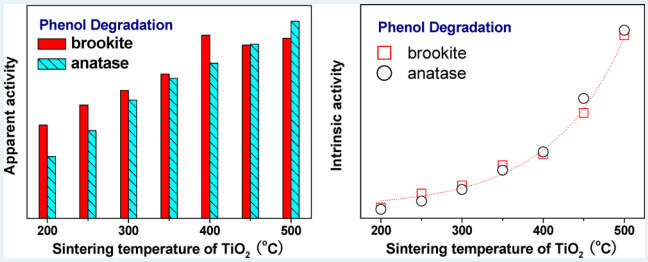


**KEYWORDS:** *brookite, anatase, photocatalysis, phenol degradation, chromate reduction*

## 1. INTRODUCTION

Photocatalysis of $TiO_2$ for environmental remediation has been studied for more than 30 years.[1−5] It is recognized that a variety of organic compounds can degrade into $CO_2$ and small fragments at ambient temperature and pressure only using $O_2$ as an oxidant. The reaction is initiated by the band gap excitation of $TiO_2$, followed by generation of various reactive species, including the conduction band electron ($e_{cb}^-$) and valence band hole ($h_{vb}^+$) of $TiO_2$ (eqs 1−8). However, the efficiency achieved so far with the $TiO_2$-based system is still not high enough to enable practical application. This is mainly because $e_{cb}^-$ and $h_{vb}^+$ easily recombine to heat, without chemical reactions with surface adsorbates. For example, Degussa P25 $TiO_2$ is a good photocatalyst, but its quantum yield for phenol degradation in aerated aqueous suspension is only 0.14 at 365 nm.[6] Although a great effort has been made in the past years, the essential factor that determines the photocatalytic activity of $TiO_2$ still remains incompletely elucidated.[3−5]

$$TiO_2 + h\nu \rightarrow e_{cb}^- + h_{vb}^+ \quad (1)$$

$$e_{cb}^- + O_2 + H^+ \rightarrow HO_2^\bullet \quad (2)$$

$$e_{cb}^- + HO_2^\bullet + H^+ \rightarrow H_2O_2 \quad (3)$$

$$2e_{cb}^- + O_2 + 2H^+ \rightarrow H_2O_2 \quad (4)$$

$$h_{vb}^+ + H_2O \rightarrow {}^\bullet OH + H^+ \quad (5)$$

$$2{}^\bullet OH \rightarrow H_2O_2 \quad (6)$$

$$H_2O_2 + h\nu \rightarrow 2{}^\bullet OH \quad (7)$$

$$H_2O_2 + e_{cb}^- + H^+ \rightarrow {}^\bullet OH + H_2O \quad (8)$$

In nature, $TiO_2$ exists in three crystal forms of anatase, rutile, and brookite, among which rutile is the mostly stable. For organic degradation in aerated aqueous solution, the apparent photocatalytic activity of anatase is usually much higher than that of rutile, whereas a mixture of anatase with rutile is more active than single phase.[7,8] Comparatively, brookite has been much less studied, due to the difficulty of its synthesis in pure crystal form. In recent years, the interest in brookite as a photocatalyst has increased.[9] However, a controversial result about its photocatalytic activity has been reported. On one hand, brookite is more active than anatase for alcohol oxidation to aldehyde in aerated aqueous solution.[10,11] On the other hand, brookite is less active than anatase for the degradation of

Received: June 7, 2014
Revised: July 24, 2014
Published: August 21, 2014

  

dichloroacetic acid (DCA), 2,4-dichlorophenol (DCP), methyl orange (MO), and rhodamine B (RhB) in aerated aqueous solution.[12−14] This discrepancy may result from changes in the physical parameters of $TiO_2$ and/or from the effect of organic photolysis, adsorption, and dye sensitization.[15] Several reports have shown that the photocatalytic activity of brookite not only changes with its sintering temperature[14,16,17] but also increases with its crystallinity or crystal size.[18,19] These observations with brookite look similar to those widely reported in the literature with anatase and rutile.[2]

In general, the catalyst activity is evaluated from the apparent rate of organic degradation in aqueous phase, without consideration of $O_2$ adsorption possibly changing with the nature of $TiO_2$. Then, the observed relative activity among the photocatalysts may be wrong, because any delay of $e_{cb}^-$ consumption by $O_2$ would inhibit further generation of $e_{cb}^-$ and $h_{vb}^+$ and consequently make the photocatalyst deactivated. In a previous study, we have found that with the same amount of $Ag^+$ on the oxide surface for phenol degradation under $N_2$, the intrinsic photocatalytic activity of $TiO_2$ only increases with its sintering temperature ($T_s$), whatever the solid is in the crystal forms of anatase, rutile, and their mixture.[20,21] Accordingly, we propose that the observed higher photoactivity of anatase than that of rutile at given $T_s$ is attributed to its larger uptake of $O_2$ from aqueous solution, whereas the mixed-phase effect is due to diffusion of the adsorbed $O_2$ from anatase to rutile. However, the intrinsic photocatalytic activity of the brookite-based $TiO_2$ has been not reported yet in the literature.

In this work, both the apparent and intrinsic photocatalytic activities of brookite and anatase have been evaluated and compared under similar conditions. The phase-pure oxides were synthesized at 200−500 °C, followed by characterization with several techniques. The catalyst activity was assessed by using phenol oxidation, chromate reduction, and $H_2O_2$ production as model reactions. The measurement was conducted in aqueous solution under UV light at wavelengths longer than 320 nm. Under these conditions, both phenol photolysis in water and its dark adsorption on $TiO_2$ were negligible. This would simplify the activity measurement, without the need to examine the effect of organic photolysis, adsorption, and dye sensitization on the rate of organic degradation. Phenol degradation was examined using $O_2$ and $Ag^+$ as electron scavengers of $TiO_2$, respectively. On the contrary, Cr(VI) anion strongly adsorbs onto $TiO_2$ in water, and it can be reduced to Cr(III) over the irradiated $TiO_2$, in accompany with $H_2O$ oxidation to $O_2$. Then the rate of Cr(VI) reduction per the amount of its adsorption would give further evidence on the intrinsic photoreactivity of $TiO_2$. On the other hand, in the aerated aqueous suspension of $TiO_2$, $H_2O_2$ can be produced through $O_2$ reduction (eqs 2−4), $H_2O$ oxidation (eqs 5 and 6), and/or both. Then, the measurement of $H_2O_2$ formation in the presence of excess hole scavenger will provide information on the fate of $O_2$ reduction and consequently on the sorption capacity toward $O_2$ in water among the different photocatalysts. Although three model reactions are different, they give similar results about the intrinsic activity of $TiO_2$. Furthermore, a plausible mechanism responsible for the observed different apparent activities of brookite and anatase is discussed.

## 2. EXPERIMENTAL SECTION

**Materials.** Titanium bis(ammonium lactate) dihydroxide (TALH), titanium tetrachloride, phenol, peroxidase (POD), and *N*,*N*-diethyl-1,4-phenylenediamine (DPD) were purchased from Sigma-Aldrich, and other reagents were purchased from Shanghai Chemicals Inc., China. Brookite $TiO_2$, denoted as sBT, was synthesized using the literature method.[12] Briefly, 36 g of urea and 10 mL of TALH were dissolved in 100 mL of water and then transferred into an autoclave, followed by heating at 160 °C for 24 h. After the reactor cooled down, the precipitates were collected by centrifugation and washed thoroughly with water and ethanol and dried at 60 °C in a vacuum oven. Anatase $TiO_2$, denoted as sAT, was prepared in an iced bath from the hydrolysis of $TiCl_4$ in the aqueous solution of $(NH_4)_2SO_4$ and HCl, followed by refluxing at 100 °C for 2 h.[22] After the suspension cooled down, its pH was adjusted to 6 with aqueous ammonia, and the solid was collected by filtration, washed thoroughly with water, and dried at 60 °C in a vacuum oven. Finally, the above prepared sBT and sAT were sintered in air at different temperatures (200−500 °C) for 3 h.

**Characterization.** X-ray diffraction (XRD) was recorded on a D/max-2550/PC diffractometer (Rigaku), using a Cu K$\alpha$ as the X-ray irradiation source. By using the Scherrer equation, the average crystallite diameters ($d_s$) for anatase, brookite, and rutile were calculated, according to the full-widths at half-maximum of (101) anatase at $2\theta$ = 25.3°, (121) brookite at $2\theta$ = 30.8°, and (110) rutile at $2\theta$ = 27.4°, respectively. Raman spectra were obtained on a Jobin Yvon LabRam 1B with a He−Ne laser excitation at 632.8 nm. Adsorption−desorption isotherms of $N_2$ on solid were measured at 77 K on a Micromeritics ASAP2020 apparatus. Then from the adsorption and desorption branches of the isotherms, the Brunauer−Emmett−Teller (BET) specific surface area ($A_{sp}$) and total pore volume ($V_p$) were calculated, respectively. Diffuse reflectance spectrum was recorded on a Shimadzu UV-2550 with $BaSO_4$ as a reference. The reflectance ($R$) was transferred into the Kubelka−Munk (K−M) absorbance, $F_R = (1-R)^2/(2R)$. The indirect band gap energy ($E_g$) of $TiO_2$ was estimated following the equation, $[F_R \cdot E_{hv}]^{0.5} = E_{hv} - E_g$, where $E_{hv}$ represents light energy.[23]

**Photocatalysis.** Reactions were carried out under constant magnetic stirring in a Pyrex-glass reactor (inner size, 2.9 cm × 9.1 cm), attached with a water jacket thermostated at 25 °C. The distance between the reactor and lamp was fixed at 10 cm. Light source was a 375 W high pressure mercury lamp (Shanghai Mengya, China). The light intensity reaching the external surface of the reactor was 4.8 mW/cm$^2$, measured by a UV-A irradiance meter (Instruments of Beijing Normal University, China). An aqueous suspension (50.0 mL) containing the necessary components (1.0 g/L catalyst, 0.43 mM phenol, 1.0 mM $AgNO_3$, and 0.29 mM chromate) was stirred in the dark for 2 h and then irradiated with UV light. For the reaction in the presence of $AgNO_3$, the suspension was purged with $N_2$ (99.99%) for 0.5 h and then sealed for experiments. At given intervals, 3.0 mL of the suspension was withdrawn by a microsyringe, filtered through a membrane (0.22 $\mu$m in pore size), and immediately analyzed as described below.

Phenol was analyzed by HPLC (high performance liquid chromatography) on a Dionex P680 (Apollo C18 reverse column, and 50% $CH_3OH/H_2O$ as an eluent). $H_2O_2$, chromate, and silver ions were measured on an Agilent 8451 spectrometer, through the POD-catalyzed oxidation of DPD at 551 nm,[24] through a Cr(VI) complex with 1,5-diphenylcarbazide at 540 nm,[25] and through a Ag(I) complex


dx.doi.org/10.1021/cs500785z | ACS Catal. 2014, 4, 3273−3280

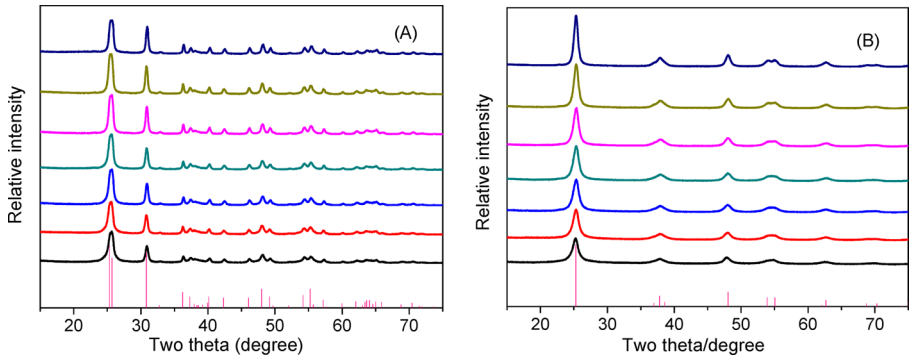


**Figure 1.** XRD patterns of (A) sBT and (B) sAT, sintered at 200, 250, 300, 350, 400, 450, and 500 °C (from bottom to top). The column plots are cited from the standard data of (A) brookite (PDF no. 29-1360) and (B) anatase (PDF no. 12-1272).

**Table 1. Physical Parameters of sBT and sAT Prepared at Different Temperatures**[a]

| | brookite | | | | anatase | | | |
|---|---|---|---|---|---|---|---|---|
| $T_s$ (°C) | $d_s$ (nm) | $A_{sp}$ ($m^2$/g) | $V_p$ ($cm^3$/g) | $E_g$ (eV) | $d_s$ (nm) | $A_{sp}$ ($m^2$/g) | $V_p$ ($cm^3$/g) | $E_g$ (eV) |
| 200 | 18.0 | 139.3 | 0.250 | 3.24 | 7.5 | 168.1 | 0.233 | 3.22 |
| 250 | 18.7 | 102.6 | 0.245 | 3.21 | 8.1 | 139.1 | 0.257 | 3.23 |
| 300 | 19.4 | 89.4 | 0.254 | 3.22 | 8.2 | 142.1 | 0.247 | 3.22 |
| 350 | 19.6 | 90.2 | 0.246 | 3.24 | 8.5 | 116.5 | 0.231 | 3.22 |
| 400 | 21.1 | 61.4 | 0.242 | 3.26 | 9.2 | 113.7 | 0.203 | 3.24 |
| 450 | 21.5 | 52.9 | 0.233 | 3.26 | 10.6 | 103.2 | 0.263 | 3.23 |
| 500 | 22.8 | 47.6 | 0.246 | 3.25 | 12.2 | 68.3 | 0.242 | 3.23 |

[a]Values for $T_s$, sintering temperature; $d_s$, crystal size, calculated with the (121) brookite or with the (101) anatase; $A_{sp}$, the BET surface area; $V_p$, total pore volume; $E_g$, indirect band gap energy.

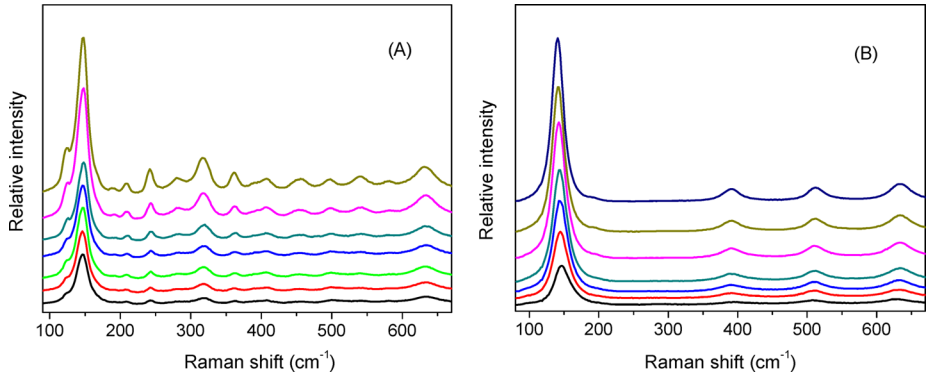


**Figure 2.** Raman spectra of (A) sBT and (B) sAT, sintered at 200, 250, 300, 350, 400, 450, and 500 °C (from bottom to top).

with *p*-dimethylaminobenzalrhodanine at 468 nm,[26] respectively.

## 3. RESULTS AND DISCUSSION

**Characterization.** The crystal structures of sBT and sAT were confirmed by XRD and Raman spectroscopy. Figure 1 shows the XRD patterns of samples sintered at different $T_s$. The diffraction pattern of sBT was in good agreement with that of brookite (PDF no. 29-1360), while sAT showed a typical pattern of anatase (PDF no. 12-1272). No other crystalline phases were found with all the samples. As $T_s$ increased, the diffraction intensity and peak width for sBT or sAT increased and decreased, respectively. This is indicative of the growth of brookite crystals in sBT and of anatase crystals in sAT, respectively. By using the Scherrer equation, the average crystal diameters were calculated, which progressively increases with $T_s$ for both sBT and sAT (Table 1). Moreover, the estimated lattice parameters and cell volumes of sBT and sAT were not only nearly independent of $T_s$ but also very close to those recorded with bulk brookite and anatase in database, respectively (Tables S1 and S2, Supporting Information).

However, the diffraction peaks of anatase and brookite largely overlap. Then it is hard to identify whether anatase phase is also present in sBT. The solid was then characterized with Raman spectroscopy, and the results are shown in Figure 2. The lattice of brookite $TiO_2$ has a $D_{2h}^{15}$ symmetry.[27] According to group theory, there are 69 optical modes ($9A_{1g}$ + $9B_{1g}$ + $9B_{2g}$ + $9B_{3g}$ + $9A_{1u}$ + $8B_{1u}$ + $8B_{2u}$ +$8B_{3u}$), among which, only $A_{1g}$, $B_{1g}$, $B_{2g}$, and $B_{3g}$ are Raman active.[27] With sBT, there were 14 Raman bands in the range from 100 to 700 $cm^{-1}$, which can be assigned to $A_{1g}$ (122, 148, 188, 243, 406, 541, and 632 $cm^{-1}$), $B_{1g}$ (211, and 280 $cm^{-1}$), $B_{2g}$ (363, 459, and 582 $cm^{-1}$), and $B_{3g}$ (320, and 498 $cm^{-1}$) of brookite. Importantly, the Raman vibrations characteristic of anatase at 512 $cm^{-1}$ and of rutile at 442 $cm^{-1}$ were absent with all sBT samples. In respect of sAT, there were 4 Raman bands around 142, 390,


dx.doi.org/10.1021/cs500785z | ACS Catal. 2014, 4, 3273−3280

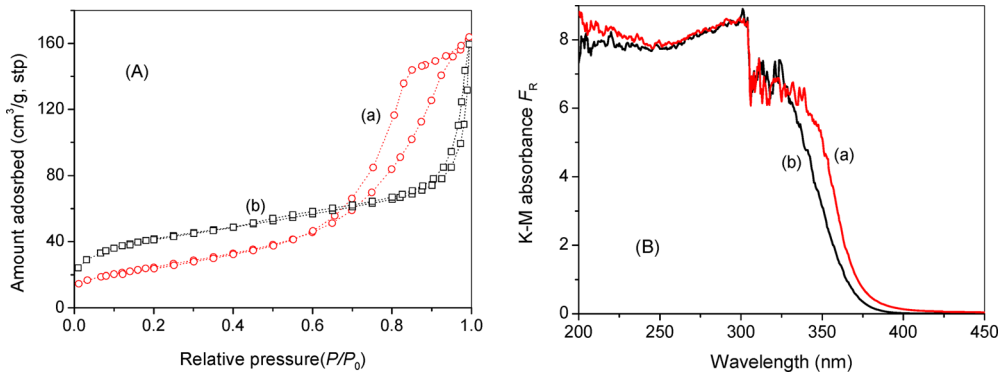


**Figure 3.** (A) Adsorption−desorption isotherms of $N_2$ at 77 K on (a) sBT and (b) sAT and (B) diffuse reflectance spectra of (a) sBT and (b) sAT. Both the oxides were prepared at 300 °C.

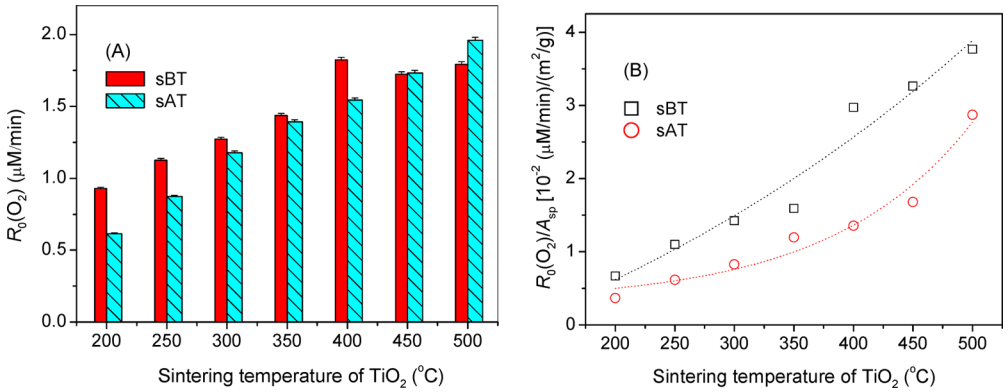


**Figure 4.** (A) Initial rate of phenol photodegradation [$R_0(O_2)$], measured in an aerated aqueous suspension. (B) The normalized $R_0(O_2)$ with $A_{sp}$, the BET surface area of $TiO_2$.

512, and 634 $cm^{-1}$, which can be assigned to $E_g$, $B_{1g}$, $A_{1g}$, and $E_g$ of anatase, respectively.[28,29] The typical vibration of rutile at 442 $cm^{-1}$ was also absent with all sAT samples. These observations confirm that all the samples of anatase and brookite synthesized in this work are in pure crystal forms. Moreover, for both sBT and sAT, the Raman peak width and integrated intensity around 150 $cm^{-1}$ decreased and increased with the increase of $T_s$, respectively (Tables S3). This observation indicates that the crystal size and crystallinity of brookite in sBT and of anatase in sAT increase with $T_s$, the trend in good agreement with that from XRD analysis.

Furthermore, $N_2$ adsorption isotherms and UV−vis diffuse reflectance spectra of all samples were also measured. Figure 3 shows the results of two representative samples sintered at 350 °C. The isotherm of sAT was Type I, while the isotherm of sBT was Type IV. This is indicative of micropores and mesopores present in sAT and sBT, respectively. However, as $T_s$ increased, the isotherm of sAT changed to a Type IV, while the hysteresis loop of sBT shifted toward the high pressure side (Figure S1). Because of that, there was a wide distribution in the BJH pore size, from 17 to 150 nm for sAT and from 14 to 300 nm for sBT. A *t*-plot analysis showed that sAT had notable micropores (0.046 $cm^3/g$ at 200 °C, and the volume then decreased sharply with $T_s$), while sBT had negligible micropore volume at $T_s$ < 350 °C. These observations indicate that the solids undergo a complicated reconstruction of porous networks on the thermal treatment. As a result, the total pore volume slightly changed with $T_s$, while sAT and sBT had similar total pore volume at given $T_s$ (Table 1). On the other hand, the BET surface area gradually decreased with $T_s$, while sAT always had a larger surface area than sBT (Table 1). Since $N_2$ largely adsorbs onto the external surface of the solid, this observation indicates that the particle size of sAT is smaller than that of sBT at given $T_s$, while the particle size of both sAT and sBT increases with $T_s$. With respect to the solid absorption spectrum, there was a strong band in the wavelength region from 200 to 400 nm (Figure 3B), due to the ligand-to-metal charge transfer ($O^{2-}$ to $Ti^{IV}$). Through a Tauc plot (Figure S3), the band gap energy ($E_g$) for the indirect transition was estimated, which was 3.24 ± 0.02 eV for sBT and 3.23 ± 0.01 eV for sAT. These values of $E_g$ are nearly independent of $T_s$ (Table 1), indicating that both sBT and sAT are bulk $TiO_2$, in agreement with the result of lattice parameters above. However, at a wavelength longer than 320 nm, the K−M absorbance of sBT was somewhat larger than that of sAT at given $T_s$ (Figure S2). The exact reason for that is not known, but it may relate to the fact that brookite has a large unit cell (256.0 ± 0.05 $Å^3$) and a high density of $TiO_2$ (4.120 $cm^3/g$), as compared to those of anatase (136.8 ± 0.05 $Å^3$ and 3.893 $cm^3/g$). A larger unit cell and higher density of $TiO_2$ may intercept a greater number of the photons reaching the solid powders. The above information on the physical properties of $TiO_2$ would be useful to the following study of $TiO_2$ photocatalysis.

**Photodegradation of Phenol.** The reactions were carried out under UV light using $O_2$ and $Ag^+$ as oxidants, respectively. It is known that in the aerated aqueous suspension of $TiO_2$, the apparent rate of phenol degradation is first order in phenol; but in the $N_2$-purged aqueous suspension of $TiO_2$ and $AgNO_3$, phenol degradation falls to follow the first-order kinetics, due to the reduction of Ag(I) to Ag by $e_{cb}^-$ of $TiO_2$, and thus to the


dx.doi.org/10.1021/cs500785z | ACS Catal. 2014, 4, 3273−3280

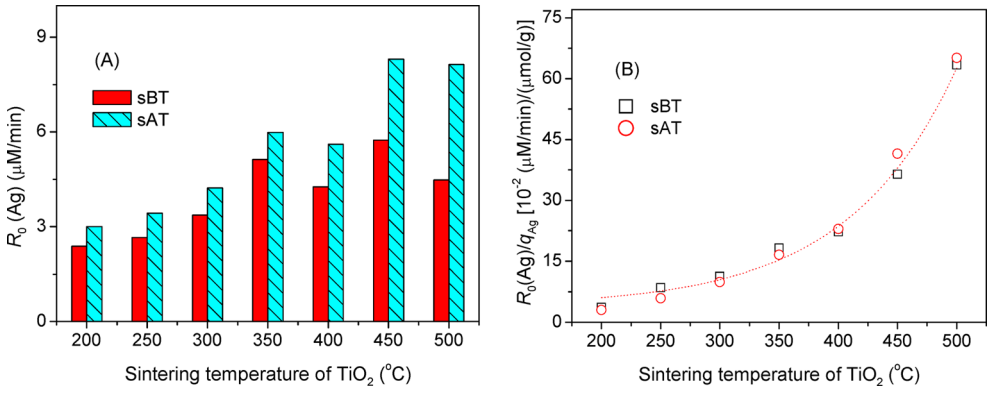


**Figure 5.** (A) Initial rate of phenol photodegradation [$R_0$(Ag)], measured in a $N_2$-purged aqueous suspension containing 1.0 mM $AgNO_3$. (B) The normalized $R_0$(Ag) with $q_{Ag}$, the initial amount of $Ag^+$ adsorbed on $TiO_2$, measured in the dark and before light irradiation.

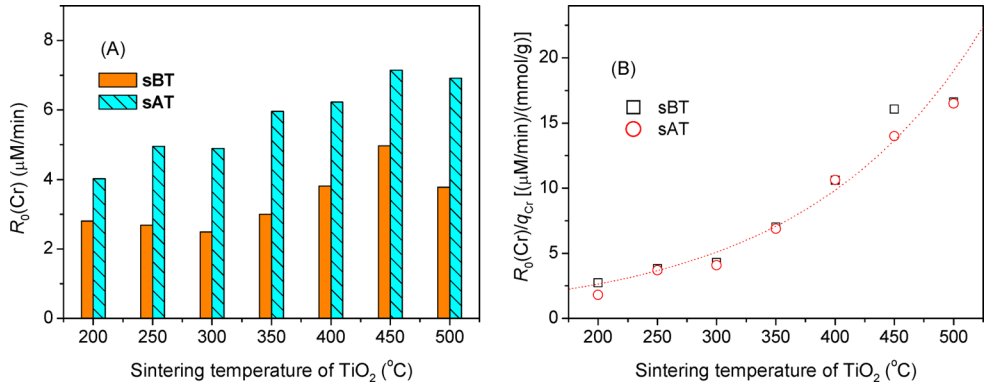


**Figure 6.** (A) Initial rate of Cr(VI) reduction [$R_0$(Cr)] in an aerated aqueous suspension and (B) the normalized $R_0$(Cr)] with $q_{Cr}$, the initial amount of Cr (VI) adsorbed on $TiO_2$, measured in the dark and before light irradiation.

decrease of Ag(I) concentration with time.[20] Therefore, in this study, only the initial rate of phenol degradation in the first 10 min has been measured and then used as a measure of the relative activity among different catalysts.

Figure 4A shows the results of phenol degradation measured in an aerated aqueous suspension. With sBT or sAT, the initial rate of phenol degradation [$R_0(O_2)$] was a function of $T_s$. However, sBT was more and less active than sAT at a sintering temperature lower and higher than 450 °C, respectively. The former observation is similar to those reported with alcohol oxidation,[9,10] while the latter is similar to those reported for DCA, DCP, MO, and RhB degradation.[11−13] In the literature, the apparent rate of organic degradation is often normalized with the BET surface area of the catalyst ($A_{sp}$), considering that all surface area may have taken part in the photocatalytic reaction.[1−5] According to this specific rate of phenol degradation [$R_0(O_2)/A_{sp}$], the activity of sBT was always higher than that of sAT (Figure 4B). Since phenol adsorption on $TiO_2$ in water was rather weak (less than 3%), this observation implies that sBT and sAT may have different sorption capacities toward the dissolved $O_2$ in water. However, it is difficult to measure the amount of $O_2$ adsorption on solid in solution. In the following, $Ag^+$ will be used as an alternative oxidant, because its adsorption on $TiO_2$ in water can be easily quantified. This effort is to assess the catalyst activity with the same amount of electron acceptor ($O_2$) on the different catalysts.

Figure 5A shows the results of phenol degradation, measured in the $N_2$-purged aqueous solution of $TiO_2$ and $AgNO_3$. Before light irradiation, the amount of Ag(I) adsorbed on each oxide in water ($q_{Ag}$) was measured (Figure S4A). With sBT or sAT, the initial rate of phenol degradation [$R_0$(Ag)] was a function of $T_s$. However, the value of $R_0$(Ag) obtained with sBT was always lower than that measured with sAT at given $T_s$. Control experiments in the dark or in the absence of $TiO_2$ showed negligible phenol degradation. Since phenol degradation is the outcome of Ag(I) reduction, the value of $R_0$(Ag) was then normalized with $q_{Ag}$ (Figure 5B). With the same amount of $Ag^+$ adsorbed on the oxide surface, the intrinsic photocatalytic activities of sBT and sAT not only increased with $T_s$ but also became very close at given $T_s$. These results obtained here with brookite and anatase are similar those reported previously with anatase and rutile.[20,21] In other words, the intrinsic photocatalytic activity of $TiO_2$ exponentially increases with $T_s$, regardless of the solid structures in the forms of anatase, rutile, and brookite.

**Photoreduction of Cr(VI).** In the presence of $AgNO_3$, the observed phenol degradation under $N_2$ is due to its oxidation by $h_{vb}^+$ or $^{\bullet}OH$ on $TiO_2$ (eq 5). Although phenol adsorption on $TiO_2$ in water was very low, such weak adsorption may differ from one catalyst to another, consequently influencing the activity assessment. It is known that chromate can be reduced to Cr(III) by $e_{cb}^-$ of $TiO_2$, together with $H_2O$ oxidation to $O_2$ by $h_{vb}^+$ of $TiO_2$.[30−32] Then, the initial rate of Cr(VI) photoreduced [$R_0$(Cr)], per the initial amount of Cr(VI) adsorbed ($q_{Cr}$), would provide further information on the intrinsic photocatalytic activity of $TiO_2$.


dx.doi.org/10.1021/cs500785z | ACS Catal. 2014, 4, 3273−3280

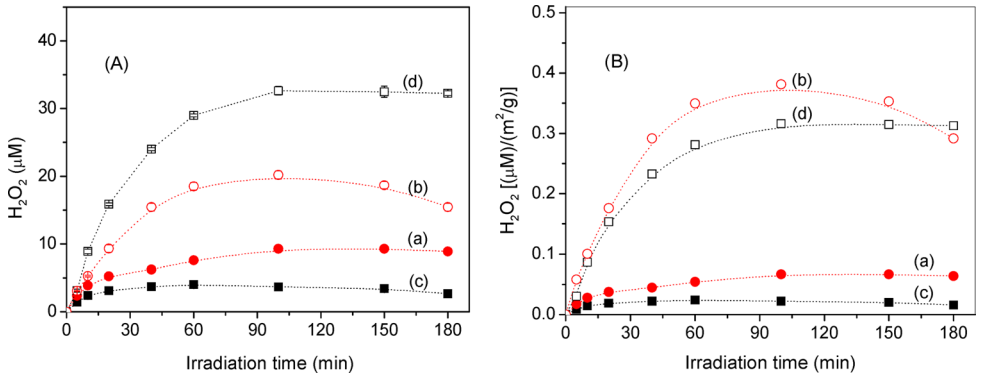


**Figure 7.** (A) Production of $H_2O_2$ in an aerated aqueous suspension containing 0.43 mM phenol. (B) The BET surface area normalized concentration of $H_2O_2$. Catalysts were (a) sBT sintered at 200 °C, (b) sBT sintered at 450 °C, (c) sAT sintered at 200 °C, and (d) sAT sintered at 450 °C.

Figure 6 shows the results of chromate photoreduction in the aerated aqueous suspension of $TiO_2$. It is known that the rate of Cr(VI) reduction is affected by Cr(III) but not by $O_2$.[30,31] To minimize the detrimental effect of Cr(III), the initial rate of Cr(VI) reduction was measured only at the first 10 min. With sBT or sAT, the value of $R_0$(Cr) was a function of $T_s$, while at given $T_s$ sAT was always more active than sBT. Since the catalysts had different values of $q_{Cr}$ (Figure S4B), the value of $R_0$(Cr) was then normalized with $q_{Cr}$, measured before light irradiation. According to this specific rate of Cr(VI) reduction (Figure 6B), the activities of sBT and sAT increased with $T_s$, the trend similar to that observed from phenol degradation (Figure 5B). Therefore, it can be concluded that the intrinsic photocatalytic activities of brookite and anatase are similar at given $T_s$, either for chromate reduction or for phenol oxidation in aqueous solution.

It is worth noting that both the values of $q_{Cr}$ and $q_{Ag}$ decrease with $T_s$, whereas at given $T_s$, sAT has a larger value of $q_{Cr}$ or $q_{Ag}$ than that of sBT (Figure S4). Since Cr(VI) anions and $Ag^+$ cations mainly adsorb onto the $OH^-$ sites of $TiO_2$ in water through an electrostatic interaction,[30−33] it follows that the number of $OH^-$ groups on sBT or sAT decreases with $T_s$ and that sAT has a greater number of $OH^-$ groups than sBT at given $T_s$. In aqueous solution at a pH lower than 6.8, the surface of $TiO_2$ is positively charged,[1,2] beneficial to the particle dispersion in water. In this regard, sAT particles would easily disperse into water, harvesting a greater number of the photons entering the reactor, as compared to sBT particles. This increased light absorption of sAT may counteract its low absorptivity toward the UV light at wavelengths longer than 320 nm (Figures 3B and Figure 3S). As a result, sAT may show similar intrinsic photocatalytic activity to sBT at given $T_s$, as observed in Figures 5B and 6B. Nevertheless, the exact light intensity absorbed by the dispersed $TiO_2$ particles in water should be measured. However, this measurement is difficult, which is a common problem in heterogeneous photocatalysis.[6] The particles dispersed in water would have different absorption spectra than those particles in a dry form, at least due to the different degree of particle aggregation.

**Photogeneration of $H_2O_2$.** Figure 7A shows the results of $H_2O_2$ formation, measured in aerated aqueous suspensions containing excess phenol (0.43 mM). Under UV light, both sBT and sAT were capable of $H_2O_2$ production, and their apparent activities increased with $T_s$. However, sBT was more active than sAT at 200 °C but less active than sAT at 450 °C. Since the intrinsic photocatalytic activity of $TiO_2$ is determined by $T_s$, the observed apparent activity difference between sBT and sAT might be due to the effect of surface area. For this concern, the amount of $H_2O_2$ ($[H_2O_2]$) produced at a given time was normalized with the BET surface area of $TiO_2$ ($A_{sp}$, Table 1), and the result is shown in Figure 7B. According to this specific value of $H_2O_2$ formation, sBT was more active than sAT either at 200 or 450 °C (Figure 7B). Interestingly, this result, obtained from $H_2O_2$ production in the presence of hole sacrifice, is in good agreement with that measured from phenol degradation in an aerated aqueous solution (Figure 4B). In other words, the reduction of $O_2$ to $H_2O_2$ is the rate-determining step for phenol degradation. Since the effect of surface area has been considered, we propose that brookite has a strong affinity to $O_2$ in water than anatase. Because of that, both the surface area normalized rates of $H_2O_2$ production and phenol degradation on sBT are larger than those on sAT at given $T_s$ (Figures 4B and 7B). Note that the observed decrease of $[H_2O_2]$ with time is indicative of $H_2O_2$ consumption through different pathways, such as direct photolysis, and reaction with $e_{cb}^-$ on $TiO_2$ (eqs 7 and 8).

**Possible Mechanism.** The one-electron reduction of $O_2$ by $e_{cb}^-$ on sBT or on sAT is allowed in thermodynamics. It has been reported that the conduction band edge potentials ($E_{cb}$) for brookite and anatase in aqueous solution at pH 0 are approximately −0.24 and −0.10 V versus normal hydrogen electrode (NHE), respectively.[12] These values of $E_{cb}$ are all more negative than that potential for the reduction of $O_2$ to $HO_2^\bullet$ (−0.05 V vs NHE). On the other hand, the valence band edge potential ($E_{vb}$) of a semiconductor can be calculated using the equation of $E_g = E_{vb} - E_{cb}$. According to the measured $E_g$ in Table 1, the calculated values of $E_{vb}$ for brookite and anatase in aqueous solution at pH 0 are 3.00 and 3.13 V vs NHE, respectively. These values of $E_{vb}$ are all more positive than the potential for $H_2O$ oxidation to $^\bullet OH$ (2.80 V vs NHE). In other words, both brookite and anatase are capable of $O_2$ reduction to $HO_2^\bullet$ and of $H_2O$ oxidation to $^\bullet OH$ at the same time. In this regard, they would be excellent photocatalysts for environmental remediation.

In the present case, phenol has one-electron redox potential of 1.44 V vs NHE in aqueous solution at pH 0,[34] and thus it can be oxidized by both $h_{vb}^+$ and $^\bullet OH$ on $TiO_2$. The formation of $H_2O_2$ on brookite and anatase is probably ascribed to two one-electron reductions of $O_2$ (eqs 2 and 3) rather than one two-electron reduction of $O_2$ (eq 4). Since $e_{cb}^-$ and $h_{vb}^+$ are generated in a pair, enrichment of $O_2$ on $TiO_2$ from water would not only increase the rate of $O_2$ reduction but also


dx.doi.org/10.1021/cs500785z | ACS Catal. 2014, 4, 3273−3280

improve the efficiency of charge separation on the irradiated $TiO_2$. Although the surface area of sBT at 500 °C is about 49% lower than that of sAT (Table 1), sBT shows a higher apparent activity than sAT, for phenol degradation in aerated aqueous solution (Figure 4A).

The reduction of $Ag^+$ to Ag on the irradiated $TiO_2$ is one-electron transfer process. Since $Ag^+$ is a stronger one-electron oxidant than $O_2$ [$E^o$ ($Ag^+$/Ag) = 0.77 V vs NHE], the initial rate of phenol degradation in the presence of $AgNO_3$ (Figure 5) is larger than that in the presence of $O_2$ (Figure 4). By using electron paramagnetic resonance spectroscopy, Litter and co-workers propose that the reduction of Cr(VI) to Cr(III) on the irradiated $TiO_2$ is a sequential one-electron-transfer process.[32] Because the one-electron redox potential of Cr(VI) (+0.6 V vs NHE) is more positive than that of $O_2$, the presence of $O_2$ in the suspension has no effect on the rate of chromate reduction.[30,31] Then, for assessment of the intrinsic photocatalytic activity of $TiO_2$, both $Ag^+$ and chromate ions as electron scavengers are appropriate to mimic $O_2$ reduction. However, as $T_s$ increases, the magnitude of the activity increase for the reaction of Cr(VI) reduction and water oxidation (Figure 6B) is lower than that obtained from the reaction of Ag(I) reduction and phenol degradation (Figure 5B). The exact reason for that is not known at the present; but it might be due to the fact that chromate ions are yellow in color, which may shield the incident photons reaching $TiO_2$. Recall that the value of $q_{Cr}$ decreases with $T_s$ (Figure S4B). Then the amount of Cr(VI) remaining in solution would increase with $T_s$. This would result in reduction in the number of photons absorbed by $TiO_2$ and consequently in the rate of Cr(VI) reduction. On the contrary, silver ions in acidic aqueous solutions are colorless and would have no effect on the band gap excitation of $TiO_2$. In this regard, to evaluate the intrinsic photocatalytic activity of $TiO_2$ for organic degradation, $Ag^+$ would be better than chromate as electron acceptors.

## 4. CONCLUSIONS

In this work, phase-pure brookite and anatase $TiO_2$ have been synthesized at 200−500 °C and examined as photocatalysts for phenol degradation, chromate reduction, and $H_2O_2$ formation. Depending on $T_s$ and the model reaction used, the apparent activity of brookite can be higher and lower than that of anatase. However, with the same amount of Ag(I) or Cr(VI) on the oxide surface, the intrinsic activity of brookite for phenol degradation or for Cr(VI) reduction become similar at given $T_s$. Importantly, such the intrinsic activities of brookite and anatase exponentially increase with the increase of $T_s$. Through measurement of $H_2O_2$ production, it is proposed that brookite has a stronger affinity to $O_2$ in water than anatase. Accordingly, the observed apparent activity of brookite different from that of anatase for organic degradation is ascribed to the combined effects of $T_s$, surface area, and sorption capacity toward the dissolved $O_2$ in water. It is recommended that brookite is a better photocatalyst than anatase for environmental use. On the other hand, the intrinsic activity of brookite that exponentially increases with $T_s$ might be due to the growth of brookite crystallites and to the formation of surface defects, as reported recently with anatase.[35] However, a further study is needed to deeply understand the origin of $T_s$ effect.

## ■ ASSOCIATED CONTENT

### Supporting Information

XRD and Raman data, $N_2$ adsorption isotherms and pore analysis, UV−vis diffuse reflectance spectra, Tauc plots, $Ag^+$ and chromate adsorption data. This material is available free of charge via the Internet at http://pubs.acs.org.

## ■ AUTHOR INFORMATION

### Corresponding Author

*E-mail: xuym@zju.edu.cn.

### Notes

The authors declare no competing financial interest.

## ■ ACKNOWLEDGMENTS

This work was supported by the 973 program of China (No. 2011CB936003) and NSFC (No. 21377110).

## ■ REFERENCES

(1) Hoffmann, M. R.; Martin, S. T.; Choi, W.; Bahnemann, D. W. *Chem. Rev.* **1995**, *95*, 69−96.
(2) Carp, O.; Huisman, C. L.; Reller, A. *Prog. Solid State Chem.* **2004**, *32*, 33−177.
(3) Tachikawa, T.; Fujitsuka, M.; Majima, T. *J. Phys. Chem. C* **2007**, *111*, 5259−5275.
(4) Kumar, S. G.; Devi, L. G. *J. Phys. Chem. A* **2011**, *115*, 13211−13241.
(5) Ryu, J.; Choi, W. *Environ. Sci. Technol.* **2008**, *42*, 294−300.
(6) Emeline, A. V.; Zhang, X.; Jin, M.; Murakami, T.; Fujishima, A. *J. Phys. Chem. B* **2006**, *110*, 7409−7413.
(7) Ohtani, B.; Ogawa, Y.; Nishimoto, S. *J. Phys. Chem. B* **1997**, *101*, 3746−3752.
(8) Hurum, D. C.; Agrios, A. G.; Gray, K. A.; Rajh, T.; Thurnauer, M. C. *J. Phys. Chem. B* **2003**, *107*, 4545−4549.
(9) Di Paola, D.; Bellardita, M.; Palmisano, L. *Catalysts* **2013**, *3*, 36−73.
(10) Augugliaro, V.; Loddo, V.; López-Muñoz, M.; Márquez-Álvarez, C. *Photochem. Photobiol. Sci.* **2009**, *8*, 663−669.
(11) Kandiel, T. A.; Robben, L.; Alkaim, A.; Bahnemann, D. W. *Photochem. Photobiol. Sci.* **2013**, *12*, 602−609.
(12) Kandiel, T. A.; Feldhoff, A.; Robben, L.; Dillert, R.; Bahnemann, D. W. *Chem. Mater.* **2010**, *22*, 2050−2060.
(13) Jiao, Y.; Chen, F.; Zhao, B.; Yang, H.; Zhang, J. *Colloids Surf., A* **2012**, *402*, 66−71.
(14) Zhang, J.; Yan, S.; Fu, L.; Wang, F.; Yuan, M.; Luo, G.; Xu, Q.; Wang, X.; Li, C. *Chin. J. Catal.* **2011**, *32*, 983−991.
(15) Lü, X.; Mao, D.; Wei, X.; Zhang, H.; Xie, J.; Wei, W. *J. Mater. Res.* **2013**, *28*, 400−404.
(16) Kominami, H.; Ishii, Y.; Kohno, M.; Konishi, S.; Kera, Y.; Ohtani, B. *Catal. Lett.* **2003**, *91*, 41−47.
(17) Štengl, V.; Králová, D. *Mater. Chem. Phys.* **2011**, *129*, 794−801.
(18) Štengl, V.; Bakardjieva, S.; Murafa, N.; Šubrt, J.; Měšťánková, H.; Jirkovský, J. *Mater. Chem. Phys.* **2007**, *105*, 38−46.
(19) Xie, J.; Lü, X.; Liu, J.; Shu, H. *Pure Appl. Chem.* **2009**, *81*, 2407−2415.
(20) Sun, Q.; Xu, Y. *J. Phys. Chem. C* **2010**, *114*, 18911−18918.
(21) Cong, S.; Xu, Y. *J. Phys. Chem. C* **2011**, *115*, 21161−21168.
(22) Anpo, M.; Shima, T.; Kodama, S.; Kubokawa, Y. *J. Phys. Chem.* **1987**, *91*, 4305−4310.
(23) Grätzel, M.; Hagfeldtt, A. *Chem. Rev.* **1995**, *95*, 49−68.
(24) Bader, H.; Sturzenegger, V.; Hoigné, J. *Water Res.* **1988**, *22*, 1109−1115.
(25) Zhang, G.; Xu, Y. *Inorg. Chem. Commun.* **2005**, *8*, 520−523.
(26) Cave, G. C. B; Hume, D. N. *Anal. Chem.* **1952**, *24*, 1503−1505.
(27) Iliev, M. N.; Hadjiev, V. G.; Litvinchuk, A. P. *Vib. Spectrosc.* **2013**, *64*, 148−152.

(28) Mathpal, M. C.; Tripathi, A. K.; Singh, M. K.; Gairola, S. P.; Pandey, S. N.; Agarwal, A. *Chem. Phys. Lett.* **2013**, *555*, 182−186.
(29) Choi, H. C.; Jung, Y. M.; Kim, S. B. *Vib. Spectrosc.* **2005**, *37*, 33−38.
(30) Gimknez, J.; Aguado, M. A.; Cervera-March, S. *J. Mol. Catal. A: Chem.* **1996**, *105*, 67−78.
(31) Chenthamarakshan, C. R.; Rajeshwar, K. *Langmuir* **2000**, *16*, 2715−2721.
(32) Testa, J. J.; Grela, M. A.; Litter, M. I. *Langmuir* **2001**, *17*, 3515−3517.
(33) Kominami, H.; Murakami, S.; Kato, J.; Kera, Y.; Ohtani, B. *J. Phys. Chem. B* **2002**, *106*, 10501−10507.
(34) Li, C.; Hoffman, M. Z. *J. Phys. Chem. B* **1999**, *103*, 6653−6656.
(35) Li, Z.; Liu, R.; Xu, Y. *J. Phys.Chem. C* **2013**, *117*, 24360−24367.